Substrate Channeling and Domain−Domain Interactions in Bifunctional Thymidylate Synthase−Dihydrofolate Reductase†

Po-Huang Liang‡ and Karen S. Anderson*

Department of Pharmacology, Yale University School of Medicine, 333 Cedar Street, New Haven, Connecticut 06520-8066

Received February 9, 1998; Revised Manuscript Received June 18, 1998

ABSTRACT: The thymidylate synthase (TS) and dihydrofolate reductase (DHFR) enzymes are found on a single polypeptide chain in several species of protozoa such as the parasitic *Leishmania major*. Earlier studies with the bifunctional TS−DHFR enzyme from *L. major* have suggested that this enzyme exhibits a phenomenon known as substrate channeling [Meek, T. D., et al. (1985) *Biochemistry 24*, 678−686]. This is a process by which a metabolite or intermediate is directly transferred from one enzyme active site to the next without being released free into solution. The crystal structure for the bifunctional TS−DHFR enzyme from *L. major* was recently solved, and it was shown that the TS active site was located 40 Å from the DHFR active site [Knighton, D. R., et al. (1994) *Nat. Struct. Biol. 1*, 186−194]. On the basis of the crystal structure, a novel mechanism has been proposed for the channeling of the intermediate, dihydrofolate, from the TS active site to the DHFR active site [Knighton, D. R., et al. (1994) *Nat. Struct. Biol. 1*, 186−194]. They suggest that the dihydrofolate is transferred via an "electrostatic" channel on the protein surface which connects the two active sites. In this report, we describe the use of a rapid transient kinetic analysis in examining the kinetics of substrate channeling as well as domain−domain interactions in the bifunctional TS−DHFR from *L. major*.

Substrate channeling is a process by which two sequential enzymes in a pathway interact to transfer a metabolite (or intermediate) directly from one enzyme active site to the next without allowing free diffusion of the metabolite (*1*, *2*). Thus, channeling is thought to play an important role in metabolic regulation and cellular control of enzymatic activities. However, rigorous kinetic and structural evidence for channeling is lacking in many cases.

Tryptophan synthase from *Salmonella typhimurium*, an $\alpha_2\beta_2$ tetrameric enzyme complex, is considered the best example for substrate channeling and represents one of the few cases in which both kinetic and structural evidence for channeling exists (*3*). Tryptophan synthase catalyzes the last two reactions in the biosynthesis of the essential amino acid tryptophan. The α subunit catalyzes the aldolytic cleavage of indole 3-glycerol phosphate to indole and glyceraldehyde 3-phosphate, while the β subunit catalyzes the condensation of indole with serine in a reaction mediated by pyridoxal phosphate. The solution of the three-dimensional structure of the enzyme from *S. typhimurium* provided physical evidence for a 25 Å, hydrophobic tunnel which connects the α and β active sites (*4*). Previous structural and kinetic studies have demonstrated that the formation of an aminoacrylate adduct between serine and pyridoxal phosphate at the β subunit modulates the formation of indole at the α subunit (*5*−*8*). These data suggest that the formation of the aminoacrylate species at the β subunit induces a change in protein conformation that is transmitted to the α subunit which increases the rate of chemical catalysis involving the cleavage of indole 3-glycerol phosphate by approximately 150-fold.

Another example of an enzyme complex suggested to display channeling behavior is the bifunctional enzyme thymidylate synthase−dihydrofolate reductase (TS−DHFR)[1,2] isolated from the protozoan species *Leishmania major* (*9*−*11*). The thymidylate synthase (TS) and dihydrofolate reductase (DHFR) enzyme activities are found on a single polypeptide chain in several species of protozoa. The recently solved X-ray structure of the TS−DHFR enzyme from *L. major* revealed the presence of a type of channel very different from that observed with tryptophan synthase (*12*, *13*). In contrast to tryptophan synthase, no obvious "tunnel" is observed even though the TS and DHFR binding sites are too far apart (40 Å) to allow for the direct transfer of H_2folate without a major protein conformational rearrangement (*13*). A novel mechanism has been proposed by Knighton et al. (*14*) in which the dihydrofolate intermediate is channeled on the basis of the electrostatics at the protein surface, and a recent detailed modeling study of the TS−DHFR protein supports the concept of electrostatic channeling.

† This work was supported by NIH Grants GM45353 and GM49551 to K.S.A.

* To whom correspondence should be addressed. Telephone: (203) 785-4526. Fax: (203) 785-7670. E-mail: karen.anderson@yale.edu.

‡ Present address: Department of Macromolecular Science, SmithKline Beecham, 709 Swedeland Rd., King of Prussia, PA 19406.

[1] Abbreviations: TS, thymidylate synthase; DHFR, dihydrofolate reductase; CH_2H_4folate, methylene tetrahydrofolate; H_4folate, tetrahydrofolate; H_2folate, dihydrofolate; MTX, methotrexate; dUMP, 2′-deoxyuridine monophosphate; FdUMP, 5-fluoro-2′-deoxyuridine monophosphate.

[2] The bifunctional enzyme is sometimes referred to as DHFR−TS since the DHFR catalytic activity resides in the N-terminal portion of the protein. This paper will use the TS−DHFR designation as functionally, the substrate channeling involves movement of DHF from the TS site to the DHFR site.

S0006-2960(98)00316-X CCC: $15.00
Published on Web 08/12/1998

Scheme 1

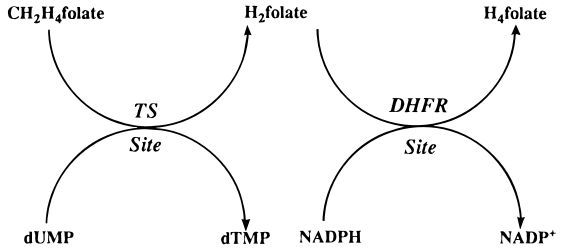

In the bifunctional enzyme, thymidylate synthase (TS) catalyzes the conversion of dUMP and (6*R*)-L-5,10-methylenetetrahydrofolate (CH_2H_4folate) to dTMP and dihydrofolate (H_2folate). The dihydrofolate reductase (DHFR) then catalyzes the subsequent reduction of H_2folate by NADPH to regenerate tetrahydrofolate (H_4folate) which is required for transfer of one carbon unit as illustrated in Scheme 1. It has been suggested that the TS and DHFR catalytic domains might communicate by transmitting protein conformational changes (*15*). Steady-state kinetic studies comparing the transient time for monofunctional forms of TS and DHFR and the bifunctional form of the TS−DHFR from methotrexate-resistant *L. major* (formerly called *Leishmania tropica*) suggest that substrate channeling of the intermediate, dihydrofolate, is occurring (*9*, *15*). More recent studies indicate that the bifunctional TS−DHFR enzyme from *Toxoplasma gondii* also exhibits channeling behavior (*16*). Although these steady-state studies indicated that channeling is occurring in the bifunctional TS−DHFR enzyme, the mechanistic details which govern the reaction kinetics for efficient channeling and domain−domain communication are not understood. In this report, we describe an in-depth transient kinetic analysis using rapid chemical quench and stopped-flow fluorescence methods to provide a quantitative description of the reaction pathway and identify essential features for efficient channeling and TS−DHFR active site communication.

Earlier studies on tryptophan synthase provide the foundation for further investigation for determining the structural and kinetic basis for efficient channeling. A detailed kinetic and structural analysis of the TS−DHFR offers a unique opportunity to compare important aspects of the kinetics of channeling and active site communication with those determined for tryptophan synthase and may reveal mechanisms common to all enzymes involved in substrate channeling.

MATERIALS AND METHODS

Enzyme. The clone of the bifunctional TS−DHFR enzyme from *L. major* was a generous gift from C.-C. Kan and D. Matthews at Agouron Pharmaceuticals. This clone harbors the pO2CLSA-4 plasmid expressed in an *Escherichia coli* Rue 10 expression vector. We obtained protein of high purity (>99%) using previously described methods for purification (*11*). The protein has both thymidylate synthase and dihydrofolate reductase activities similar to those previously reported (*9*−*11*).

Chemicals. All buffers and other reagents employed were of the highest commercial purity. Millipore ultrapure water was used for all solutions. The buffer solutions were purged with argon prior to being used. Radiolabeled and unlabeled CH_2H_4folate were prepared by the condensation of H_4folate with formaldehyde. The H_4folate was synthesized by reduction of folic acid with $NaBH_4$. The natural (6*R*)-L-CH_2H_4folate enantiomer was purified by DE-52 anion exchange chromatography (Whatman Co.) and used exclusively in the studies. H_2folate was prepared from the reduction of folate by sodium sulfite. The tritium-labeled CH_2H_4folate and H_2folate were synthesized using tritiated folic acid as a starting material. The [3′,5′,7,9-^{3}H]folic acid was obtained from Moravek Biochemicals (Brea, CA). (6*S*)-H_4folate was enzymatically prepared from H_2folate by using dihydrofolate reductase (*17*) and purified by DE-52 anion exchange chromatography.

Enzyme Assays. The DHFR activity of the bifunctional enzyme was determined by following the decrease in absorbance at 340 nm that accompanies the conversion of substrates NADPH and H_2folate to products $NADP^+$ and H_4-folate ($\Delta\epsilon = -12.8$ mM^{-1} cm^{-1}) as described previously (*9*). The TS activity was monitored by following the increase in absorbance at 340 nm that accompanies the conversion of substrates dUMP and CH_2H_4folate to dTMP and H_2folate ($\Delta\epsilon = 6.4$ mM^{-1} cm^{-1}) (*9*).

Enzyme Concentration. The protein concentration of TS−DHFR was determined spectrophotometrically at 280 nm by using a molar extinction coefficient of 67 800 M^{-1} cm^{-1}. The active site concentration of DHFR in the bifunctional TS−DHFR was determined by monitoring the decrease in protein fluorescence upon titration with methotrexate (MTX). The active site concentration of TS in TS−DHFR was determined by measuring the decrease in protein fluorescence upon titration of CH_2H_4folate in the presence of MTX and FdUMP.

Equilibrium Fluorescence Experiments. Steady-state measurements to determine the K_d for ligands at the TS site were taken using an SLM 4800 fluorimeter (Urbana, IL) at 25 °C. The excitation wavelength was 287 nm, and the emission at 340 nm was monitored over time. Active site titrations were carried out in a 3 mL quartz cuvette that was being stirred by adding ligand in small aliquots to minimize any dilution effects. Fluorescence measurements were recorded as an average of five 4 s readings within 15−30 s of ligand addition, and the recorded fluorescence intensities were corrected for dilution. The data from the active site titrations were fitted to the following expression which relates the observed fluorescence to the concentration of ligand and provides an estimate of the K_d (*18*):

$$F = F_0 + \frac{\Delta F}{[E_0]}\left[(K_d^{app} + [E_0] + [S_0]) - \sqrt{(K_d^{app} + [E_0] + [S_0])^2 - 4[E_0][S_0]}\right]/2$$

Rapid Quench Experiments. The rapid quench experiments were performed using a Kintek RFQ-3 Rapid Chemical Quench Apparatus (Kintek Instruments, State College, PA). The reaction was initiated by mixing the enzyme solution (15 μL) with the radiolabeled substrates (15 μL, approximately 20 000 dpm). In all cases, the concentrations of enzyme and substrates cited in the text are those after mixing and during the enzymatic reaction. The enzyme reaction was terminated by quenching with 67 μL of 0.78 N KOH to give a final concentration of 0.54 N KOH. Since CH_2H_4folate is more stable under basic conditions, it was

necessary to maintain a basic pH (9.5) until mixing with enzyme solution provided a final pH of 7.8 during the enzymatic reaction. Experimental mixtures involving the production of H_4folate were protected from nonenzymatic oxidation to H_2folate by the addition of 10% (w/v) sodium ascorbate and 200 mM β-mercaptoethanol to the base quench solution to prevent H_4folate degradation after the enzyme reaction is terminated. The addition of sodium ascorbate into the base quench solution results in a final pH of 12.6. The presence of sodium ascorbate in the substrate and enzyme solutions prevented the oxidation of H_4folate during the enzymatic reaction. The quenched reaction solution was directly collected into an argon-purged vial for a Waters WISP autosampler, vortexed, and analyzed by HPLC in combination with radioactivity-flow detection. The substrates and products were quantified by HPLC as described below. To ensure that the base was quenching the enzymatic reaction, a control was included with each experiment to ensure that catalysis was being terminated. This involved adding the substrate to a premixed solution of base and enzyme. Samples were collected in vials containing an argon atmosphere to protect against oxidation during analysis. Control experiments were also carried out to establish the stability of the radiolabeled substrates under the quench conditions employed. Control experiments also established that the addition of ascorbate did not affect the steady-state enzyme turnover rates for the TS or DHFR reactions.

HPLC Analysis. The substrates and products were quantified by HPLC in combination with a radioactivity-flow detector. The HPLC separation was performed using a BDS-Hypersil C18 reverse phase column (250 mm × 4.6 mm, Keystone Scientific, Bellefonte, PA) with a flow rate of 1 mL/min. An isocratic separation using a solvent system of 10% methanol in 200 mM triethylammonium bicarbonate at pH 8.0 was employed. The elution times were as follows: H_4folate, 6.5 min; H_2folate, 11 min; and CH_2H_4-folate, 13.5 min. The HPLC effluent from the column was mixed with liquid scintillation cocktail (Mono-Flow V, National Diagnostics) at flow rate of 4 mL/min. Radioactivity was monitored continuously using a Flo-One radioactivity-flow detector (Packard Instruments, Downers Grove, IL). The analysis system was automated by using a Waters 712B WISP (Milford, MA) autosampler.

Stopped-Flow Experiments. Stopped-flow measurements were performed using a Kintek SF-2001 (Kintek Instruments). This apparatus has a 1.5 ms dead time, a 0.5 cm path length, and a thermostated observation cell maintained at 25 °C. For TS, the change in protein conformation upon substrate binding was monitored by following protein fluorescence using a monochromator set at 287 nm on the input and monitoring the change in intrinsic enzyme fluorescence with an output filter at 340 nm. For DHFR, coenzyme fluorescence energy transfer experiments were carried out with a 290 nm excitation and an output filter at 450 nm. In most experiments, an average of four runs was used for data analysis and a minimum of a 5-fold excess of the variable substrate over enzyme was used to allow analysis as a pseudo-first-order rate constant. The data were collected over a given time interval by an IBM 486 computer using software provided by Kintek Instruments. Rate constants were obtained by fitting the data to a single or double exponential by nonlinear regression. The combination of rapid chemical quench and stopped-flow methods allows an accurate interpretation of absorbance and fluorescence signals.

Data Analysis. The rate constants for individual single-turnover rapid chemical quench experiments (Figures 1−3) were estimated by fitting the data to a single exponential using the curve fitting program Kaleidagraph. The stopped-flow measurements provided estimates for the association and dissociation rate constants (k_{on} and k_{off}), while the equilibrium fluorescence measurements provided the K_d values for substrate and product interaction with the enzyme. The rapid chemical quench experiments provided measurements for the chemical catalysis at the TS and DHFR sites. Using the rate constants and K_d values obtained from these measurements as well as previously determined k_{on}, k_{off}, K_m, and k_{cat} values as constraints, we then sought to provide a kinetic model that would be consistent with all the kinetic and thermodynamic measurements and that might provide insights into substrate channeling and domain−domain communication.

The KINSIM kinetic simulation program (*19*) was used to model all of the kinetic data presented in this paper. The program was modified to allow the input of data from the rapid quench experiments as *x*,*y* pairs and to calculate the sum square errors in fitting the data (*20*, *21*). The data were fit by a trial and error process, maintaining the constraints of dissociation constants measured in this study (Table 1) and in the following paper (*22*) and K_d, K_m, and k_{cat} values previously reported for CH_2H_4folate, dUMP, dTMP, H_2folate, NADPH, and H_4folate (*9*, *11*, *22*−*24*). As indicated above, the rate constants involving the chemical interconversion of CH_2H_4folate and H_2folate (the TS reaction), H_2folate and H_4folate (the DHFR reaction), and CH_2H_4folate and H_4folate (the TS−DHFR reaction) were obtained as fits to the single-turnover kinetics or measured by stopped-flow fluorescence experiments. The focus of the simulations was twofold: first, with estimates for the kinetic constants in hand, to see if substrate channeling needs to be invoked to explain all the kinetic data; and second, to predict if there may be additional kinetic features such as domain−domain interactions which may be important in substrate channeling (see the text in Results). A description of the modeling is given below. An in-depth summary is provided as Supporting Information.

The model and estimated rate constants are described in Chart 1. In this model, the reactions occurring at the TS site include the first five steps (k_1 and k_{-1} through k_5 and k_{-5}). The channeling step is represented by k_6 and k_{18}. The reactions occurring at the DHFR site are indicated by steps k_7 and k_{-7} through k_{12} and k_{-12}. These steps describe the enzyme when either the TS or DHFR reaction is occurring but not both reactions (TS−DHFR). Steps k_{13} and k_{-13} through k_{18} and k_{-18} are used to describe the enzyme when both reactions are occurring simultaneously. If it is known how fast the substrates bind and dissociate as well as the rate at which catalysis at each site occurs, the kinetic simulations allow an estimate of whether the channeling steps, k_6 and k_{18}, need to be included in the model and if so what the rate may be. The kinetic simulations (see Results) suggest that a lower limit for the rate of channeling H_2folate from the TS to the DHFR site is 1000 s^{-1}. This constraint is based upon our observation that no H_2folate accumulates during a single enzyme turnover of the TS−DHFR reaction

Chart 1

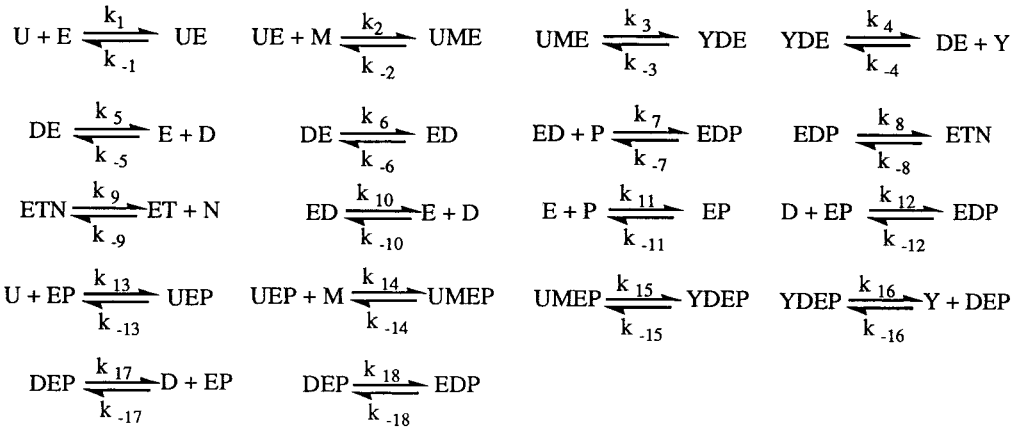

$k_1 = 15\ \mu M^{-1}s^{-1}$ $k_{-1}=3\ s^{-1}$ $k_2 = 30\ \mu M^{-1}s^{-1}$ $k_{-2} =200\ s^{-1}$ $k_3 =2.6\ s^{-1}$ $k_{-3} = 0\ s^{-1}$

$k_4 =100 s^{-1}$ $k_{-4}=10\ \mu M^{-1}s^{-1}$ $k_5 =200 s^{-1}$ $k_{-5}=3\ \mu M^{-1}s^{-1}$ $k_6=1000\ s^{-1}$ $k_{-6}=0 s^{-1}$

$k_7 =100\ \mu M^{-1}s^{-1}$ $k_{-7}=200 s^{-1}$ $k_8=14 s^{-1}$ $k_{-8}=.001 s^{-1}$ $k_9=127 s^{-1}$ $k_{-9}=47\ \mu M^{-1}s^{-1}$

$k_{10} =6.8 s^{-1}$ $k_{-10}=34\ \mu M^{-1}s^{-1}$ $k_{11}=21\ \mu M^{-1}s^{-1}$ $k_{-11}=1.8 s^{-1}$ $k_{12} =34\ \mu M^{-1}s^{-1}$ $k_{-12} =6.8 s^{-1}$

$k_{13} =15\ \mu M^{-1}s^{-1}$ $k_{-13}=3\ s^{-1}$ $k_{14} =30\ \mu M^{-1}s^{-1}$ $k_{-14}=200 s^{-1}$ $k_{15} =2.6 s^{-1}$ $k_{-15} =0 s^{-1}$

$k_{16} =100 s^{-1}$ $k_{-16}=10\ \mu M^{-1}s^{-1}$ $k_{17} =6.8\ s^{-1}$ $k_{-17}=34\ \mu M^{-1}s^{-1}$ $k_{18}=1000\ s^{-1}$ $k_{-18}=0 s^{-1}$

(within the limits of detection). If the rate of channeling was slower, for instance 100 s^{-1}, we would have observed a concentration of approximately 1 μM which is well within our detection limits. Additional information on the modeling is included as Supporting Information.

RESULTS

Equilibrium Fluorescence Measurements. The equilibrium dissociation constants (K_d) for dUMP and CH_2H_4folate binding to TS−DHFR were measured by protein fluorescence quenching using the equilibrium fluorescence titration experiments described in Materials and Methods. The plot of protein fluorescence versus [L] was fit to a quadratic equation to obtain the K_d constants. The K_d values for different substrates at 25 °C and pH 7.8 (buffer A) summarized in Table 1 are consistent with previous studies (*9*, *23*). Ligand affinity at the TS is altered by the presence of MTX at the DHFR site and is consistent with rapid chemical quench experiments (see below) which suggest that the TS site is regulated by MTX.

Table 1: Dissociation Constants for the TS Site of TS−DHFR at pH 7.8 and 25 °C

reaction	K_d (μM)
$CH_2H_4F + E \rightleftarrows E{\cdot}CH_2H_4F$	6.98 ± 1.20
$dUMP + E \rightleftarrows E{\cdot}dUMP$	0.18 ± 0.05
$CH_2H_4F + E{\cdot}MTX \rightleftarrows E{\cdot}MTX{\cdot}CH_2H_4F$	52.1 ± 4.7
$CH_2H_4F + E{\cdot}MTX{\cdot}FdUMP \rightleftarrows E{\cdot}MTX{\cdot}FdUMP{\cdot}CH_2H_4F$	4.05 ± 0.3

Scheme 2

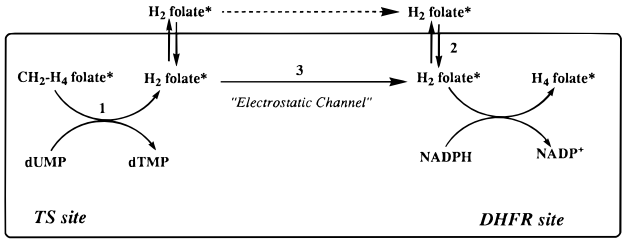

A combination of transient kinetic experiments using rapid chemical quench and stopped-flow methods has provided definitive evidence for substrate channeling and domain−domain interactions in the bifunctional TS−DHFR enzyme from *L. major*. We have previously found that the examination of a single enzyme turnover provides an important diagnostic experiment for evaluating substrate channeling as well as for detecting enzyme intermediates (*5*, *25*, *26*).

The first kinetic test of substrate channeling in TS−DHFR was to demonstrate that the product from the TS reaction, dihydrofolate (H_2folate), is directly transferred from the TS active site to the DHFR active site and not allowed to dissociate from the enzyme. This was done by a series of three single-enzyme turnover rapid chemical quench experiments as illustrated in Scheme 2.

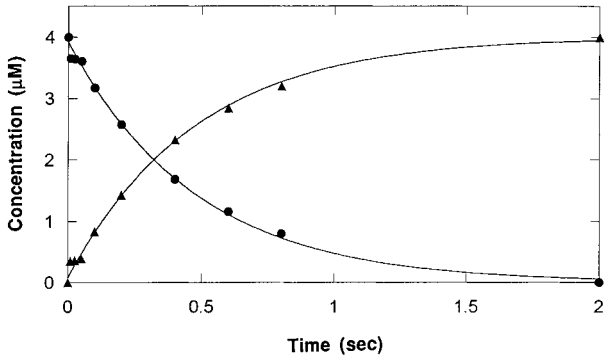

FIGURE 1: Single-turnover time course for the TS reaction. The bifunctional TS−DHFR enzyme (30 μM) preincubated with dUMP (500 μM) was mixed with (6*R*)-L-[^{3}H]CH_2H_4folate (4 μM) in the presence of $MgCl_2$ (25 mM) and EDTA (1 mM) at pH 7.8 and 25 °C. The disappearance of [^{3}H]CH_2H_4folate (●) and formation of [^{3}H]H_2folate (▲) were monitored by HPLC as described in Materials and Methods. The data were fit to a single exponential to provide a rate constant of 2.1 ± 0.07 s^{-1}. The curves were calculated by numerical integration as summarized in Materials and Methods.

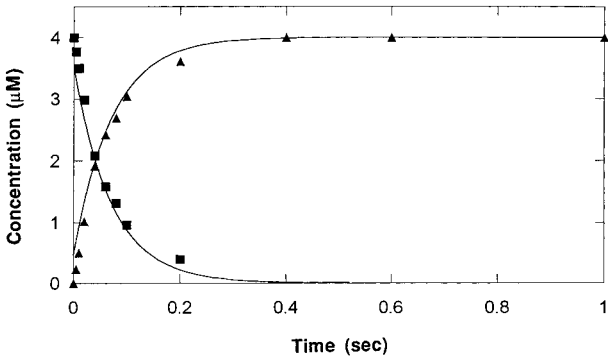

FIGURE 2: Single-turnover time course for the DHFR reaction. The bifunctional TS−DHFR enzyme (30 μM) preincubated with dUMP (500 μM) and NADPH (500 μM) was mixed with [^{3}H]H_2folate (4 μM) in the presence of $MgCl_2$ (25 mM) and EDTA (1 mM) at pH 7.8 and 25 °C. The disappearance of [^{3}H]H_2folate (■) and formation of [^{3}H]H_4folate (▲) were monitored. The data were fit to a single exponential to provide a rate constant of 14 ± 0.5 s^{-1}. The curves were calculated by numerical integration.

Single Turnover of the TS Reaction. The first experiment established the rate of catalysis of the TS reaction under single-turnover conditions designated by reaction 1 in Scheme 2. Previous steady-state kinetic studies suggest that this is an ordered reaction with dUMP binding first followed by CH_2H_4folate (*27*). The bifunctional TS−DHFR enzyme (30 μM) was preincubated with a saturating concentration of unlabeled dUMP (500 μM) and then mixed with a limiting amount of radiolabeled CH_2H_4folate (4 μM). The time course for the disappearance of CH_2H_4folate and the formation of H_2folate is shown in Figure 1. Under these conditions, the rate of catalysis was 2.1 ± 0.07 s^{-1}, similar to the steady-state turnover rate (2.6 s^{-1}), indicating that either chemical catalysis or substrate binding but not product release is rate-limiting. There was no change in the rate of catalysis under conditions in which the enzyme concentration was doubled, thus ruling out limiting substrate binding as a rate-limiting step and establishing that it is chemical catalysis which is rate-limiting under the experimental conditions employed.

Single Turnover of the DHFR Reaction. A similar set of single-turnover experiments was conducted for examining the DHFR activity of the bifunctional enzyme as designated in reaction 2 in Scheme 2. The bifunctional TS−DHFR enzyme (30 μM) was preincubated with a saturating concentration of NADPH (500 μM) and then mixed with a limiting amount of radiolabeled H_2folate (4 μM). The time course for the disappearance of H_2folate and the formation of H_4folate is shown in Figure 2. Under these conditions, the observed rate of H_4folate formation was 14 ± 0.5 s^{-1}. The same rate was observed if the enzyme was preincubated with radiolabeled H_2folate and then mixed with an excess of unlabeled NADPH (data not shown). Experiments at higher enzyme concentrations did not result in an increase in the observed rate, indicating that either chemical catalysis or product release but not substrate binding was rate-limiting. Stopped-flow fluorescence experiments (see Figure 4 below) showed no clear burst of product formation, verifying that under these conditions chemical catalysis is at least partially rate-limiting. These observations are consistent with studies on the monofunctional *E. coli* DHFR enzyme which have shown that at higher pH, the hydride transfer reaction limits chemical catalysis (*24*). These two rapid chemical quench experiments provide two important pieces of information: (1) the rate of H_2folate formation at the TS site (2.1 s^{-1}) (reaction 1 in Scheme 2) and (2) the rate of reaction of H_2-folate from solution at the DHFR site (14 s^{-1}) (reaction 2 in Scheme 2).

Single Turnover of the TS−DHFR Reaction. The third experiment was designed to directly measure the rate of conversion of CH_2H_4folate to H_2folate at the TS active site and the subsequent conversion of H_2folate to H_4folate at the DHFR active site. In principle, H_2folate may be observed as an intermediate, particularly if it must dissociate from the TS site and rebind at the DHFR site. On the other hand, if H_2folate is rapidly channeled from the TS site to the DHFR site (pathway 3 in Scheme 2), it may not be detected in the bifunctional TS−DHFR reaction.

This experiment involved measuring the rate of formation of H_4folate in the bifunctional TS−DHFR reaction using radiolabeled CH_2H_4folate substrate as illustrated by pathway 3 in Scheme 2. The bifunctional TS−DHFR enzyme (30 μM) was preincubated with a saturating concentration of unlabeled dUMP (500 μM) and NADPH (500 μM) and then mixed with a limiting amount of radiolabeled CH_2H_4folate (4 μM). The time course for the disappearance of CH_2H_4-folate and the formation of H_4folate is shown in Figure 3. Under these reaction conditions, we only observed the conversion of CH_2H_4folate to H_4folate with no H_2folate being formed as an intermediate. The data were fit to a single exponential giving a rate constant of 2.6 ± 0.1 s^{-1} which was similar to that measured for the TS reaction. Since H_2-folate was not observed as an intermediate in the TS−DHFR reaction, this indicates that either the H_2folate rapidly

Scheme 3

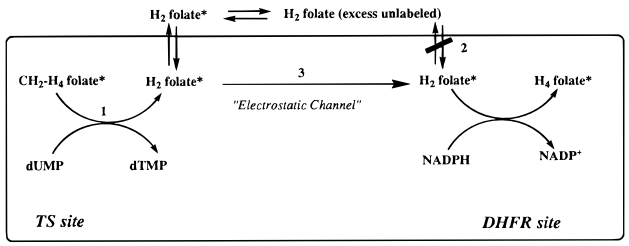

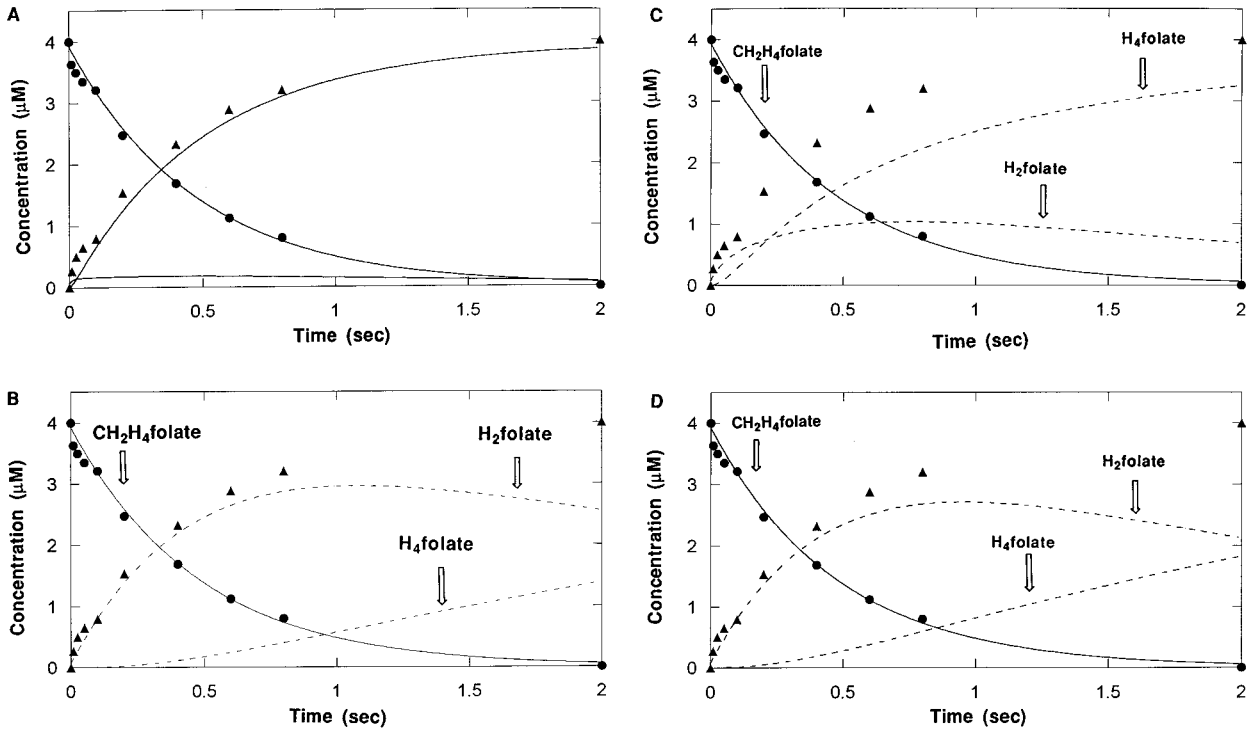

FIGURE 3: Single-turnover time course for the TS−DHFR reaction. The bifunctional TS−DHFR enzyme (30 μM) preincubated with dUMP (500 μM) and NADPH (500 μM) was mixed with [^{3}H]CH_2H_4folate (4 μM) in the presence of $MgCl_2$ (25 mM) and EDTA (1 mM) at pH 7.8 and 25 °C. The disappearance of [^{3}H]CH_2H_4folate (●) and formation of [^{3}H]H_4folate (▲) were monitored. No [^{3}H]H_2folate was detected. The data were fit to a single exponential to provide a rate constant of 2.6 ± 0.1 s^{-1}. The curves shown in panels A−D were calculated by numerical integration using KINSIM along with the rate constants and the kinetic model as described in Materials and Methods. (A) In the first simulation, both substrate channeling (at a rate of 1000 s^{-1}) and an activation of the DHFR catalytic activity (at a rate of 120 s^{-1}) are included. (B) In the second simulation, both substrate channeling and DHFR activation have been omitted. (C) In the third simulation, only substrate channeling (at a rate of 1000 s^{-1}) is included. (D) In the fourth simulation, only DHFR activation (at a rate of 120 s^{-1}) is included. In each case, the amount of H_2folate (dashed line, designated by an arrow) which would be predicted to buildup is shown. A lag in the formation of H_4folate (dashed line, designated by an arrow) is also predicted.

dissociated and rebound to the DHFR site to form H_4folate or the H_2folate was rapidly channeled to the DHFR site. The rapid dissociation and rebinding of H_2folate are less likely since we have established that the rate of reaction of H_2-folate from solution (Figure 2) is rather slow (14 s^{-1}). The absence of H_2folate as an intermediate most likely indicates that the rate of transfer from one active site to the next must be rapid. Modeling of the kinetic data using the enzyme kinetic simulation program KINSIM (*19*, *20*) provided insights into substrate channeling and domain−domain communication for the TS−DHFR reaction pathway. The rate constants and K_d values obtained from our experiments as well as previously determined k_{on}, k_{off}, K_m, and k_{cat} values were used as constraints (see Materials and Methods and Supporting Information) to develop a kinetic model that would be consistent with all the kinetic and thermodynamic measurements.

A Model for Substrate Channeling. There were two key questions to be addressed by the modeling. (1) Is a substrate channeling step required to explain the kinetic data? (2) Are there additional kinetic parameters such as domain−domain interactions which may play a role in the efficient transfer of H_2folate from the TS site to the DHFR site? A series of kinetic simulations are shown in Figure 3A−D. The reaction kinetics are most consistent with the kinetic simulation shown in Figure 3A in which a very small amount of H_2folate accumulation (within the detection limit) is predicted. We were surprised to find that simply including a substrate channeling step (>1000 s^{-1}) for the rate of transit of H_2-folate from the TS site to the DHFR site did not account for the rate of H_4folate formation and the lack of H_2folate accumulation. The simulations suggest that the rate of DHFR catalysis must be faster by 1 order of magnitude (120 s^{-1}) than the value of 14 s^{-1} measured in the DHFR reaction (Figure 2). Thus, catalysis at the DHFR site may be activated in the TS−DHFR reaction. The simulation shown in Figure 3B predicts the reaction kinetics if the substrate channeling step is omitted and the DHFR reaction occurs at 14 s^{-1} (no activation of DHFR catalysis). In this case, a large buildup of H_2folate and a substantial lag in the formation of H_4folate are predicted (dashed lines indicated by arrows). The simulation shown in Figure 3C predicts the reaction kinetics if the substrate channeling step is included and the DHFR catalysis occurs at 14 s^{-1} (no activation of DHFR catalysis). A buildup of H_2folate and lag in formation of H_4folate are predicted. The simulation in Figure 3D predicts the reaction kinetics if there is no substrate channeling but there is an activation of DHFR catalysis (120 s^{-1}). Again, a buildup of H_2folate and lag in formation of H_4folate are predicted. The results of modeling the kinetic data suggest that there is substrate channeling of H_2folate and that the DHFR catalysis may be activated in the TS−DHFR reaction perhaps by domain−domain communication. Additional experiments were required to confirm the suggestions made by modeling the kinetic data (see below).

A Pulse Chase Experiment To Test for Substrate Channeling. An additional experiment provided corroborative evidence for substrate channeling as illustrated in Scheme

3. This is a straightforward pulse chase type experiment in which enzyme is preincubated with radiolabeled CH_2H_4-folate* and NADPH and then mixed with an excess of cold dUMP and H_2folate. The rationale is as follows. If radiolabeled H_4folate* is observed, then the intermediate H_2-folate must have been channeled, because if H_2folate dissociated from the enzyme, it would have been diluted out into the pool of cold excess H_2folate preventing the observation of radiolabeled H_4folate*. In this experiment, the bifunctional TS−DHFR enzyme (30 μM) was preincubated with radiolabeled CH_2H_4folate (4 μM) and NADPH (500 μM) and then mixed with an excess of cold dUMP (500 μM) and H_2folate (25 μM). The conversion of the radiolabeled CH_2H_4folate* to H_4folate* was monitored over a period from 10 ms to 8 s (data not shown). During this time, radiolabeled CH_2H_4folate was completely converted to the product, radiolabeled H_4folate. However, under these conditions, no H_2folate was observed (within our limits of detection; >100 cpm). Thus, this pulse chase experiment provides further evidence that the H_2folate is directly channeled from the TS site to the DHFR site without being released into solution.

To provide additional evidence that H_2folate is being formed and rapidly converted to H_4folate and to exclude the possibility that H_2folate is not stable during the reaction, a more direct control experiment was carried out in which the conversion of CH_2H_4folate to H_2folate was monitored in the presence of MTX and NADPH. Under these conditions, the DHFR site would be blocked by the inhibitor, MTX, preventing DHFR catalysis and thus allowing for the observation of H_2folate. An experiment for examining a single turnover of the TS−DHFR reaction was carried out in a manner analogous to the conditions described for Figure 3 except that 150 μM MTX was included along with the bifunctional enzyme, dUMP, and NADPH. Under these experimental conditions (data not shown), the conversion of CH_2H_4folate to H_2folate was observed with no H_4folate being formed. The conversion of CH_2H_4folate to H_2folate occurred at a rate 4-fold slower (0.5 s^{-1}) than previously observed for the conversion of CH_2H_4folate. The slower rate could be the result of a reciprocal regulation of the TS site by MTX or direct occupancy of the TS active site by MTX since the concentration of MTX exceeded enzyme (30 μM). To rule out the possibility that MTX may be directly occupying the TS site. the experiment was repeated with 60 μM enzyme and 70 μM MTX. The same rate of conversion of CH_2H_4-folate to H_2folate was observed, indicating that MTX does not occupy the TS site and the reduction of the TS rate in the presence of MTX is most likely due to a regulating effect.

Scheme 4

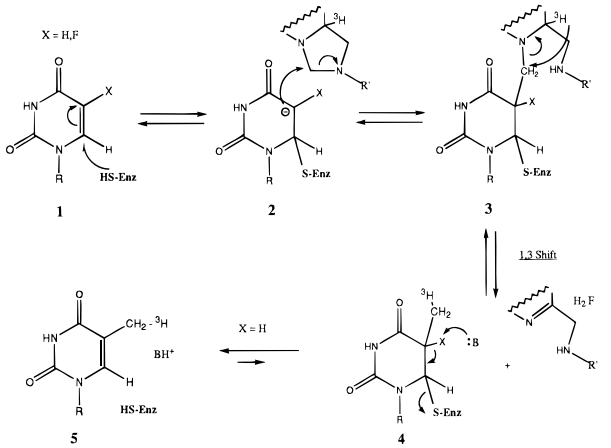

A Substrate Trapping Experiment. A substrate trapping experiment was carried out to establish that the TS reaction is indeed ordered with dUMP binding first followed by CH_2H_4folate as indicated by earlier studies (*27*). This involved an experiment in which enzyme preincubated with radiolabeled CH_2H_4folate was mixed with a large excess of unlabeled CH_2H_4folate and dUMP and the formation of radiolabeled H_2folate was monitored. No radiolabeled H_2-folate was detected, indicating that TS−DHFR binds dUMP first; thus, the radiolabeled CH_2H_4folate was diluted into the unlabeled CH_2H_4folate pool.

The combination of rapid quench experiments described above provides evidence for the substrate channeling of H_2-folate from the TS site to the DHFR site. The kinetic simulations of the data suggest that in addition the rate of DHFR catalysis must be enhanced approximately 10-fold in the TS−DHFR reaction (from 14 to 120 s^{-1}). The activation of DHFR catalysis may be required for efficient transfer of the intermediate, H_2folate, from the TS to the DHFR site site such that there is no buildup of H_2folate. Since our results suggest an enhancement in the DHFR activity under conditions in which H_2folate is channeled, it was necessary to design an experiment which directly demonstrates the predicted 10-fold activation of DHFR catalysis.

Stopped-Flow Fluorescence Studies. Stopped-flow fluorescence methods provide a convenient way of monitoring catalysis at the DHFR active site for the bifunctional TS−DHFR enzyme and of verifying rates measured using rapid chemical quench methods. In addition to standard fluorescence measurements, coenzyme fluorescence energy transfer experiments allow one to observe the conversion of NADPH to $NADP^+$ and the concomitant formation of H_4folate from H_2folate. In these experiments, the fluorescence signal measured at 450 nm is due to excitation of the dihydronicotinamide fluorescence of the coenzyme via energy transfer from the protein, and offers the advantage that only NADPH bound to enzyme is detected.

Activation of DHFR Catalysis by the TS site. The single-turnover experiment (Figure 3) which examined the TS−DHFR reaction points to a catalytic rate enhancement of the DHFR reaction when the TS site is occupied and is consistent with earlier studies which indicate domain−domain interactions in the bifunctional TS−DHFR enzyme (*15*). When an experiment is designed to demonstrate the DHFR rate enhancement for the TS−DHFR reaction under conditions where H_2folate is channeled, an ancillary issue is the actual chemical species at the TS which is responsible for this activation. A likely candidate for this chemical species is the covalent enzyme intermediate which has been shown to form during the catalysis at the TS site (as illustrated by **3** in Scheme 4). This covalent intermediate can be trapped by using the dead end inhibitor, FdUMP (*28*, *29*). Fluorescence studies on monofunctional thymidylate synthase have shown that an enzyme conformational change is associated with the formation of the covalent enzyme intermediate (*30*). Two stopped-flow experiments were carried out to look for evidence of the activation of DHFR activity by the formation of a ternary complex of TS, CH_2H_4folate, and FdUMP. In the control experiment, the enzyme (7.5 μM) was preincu-

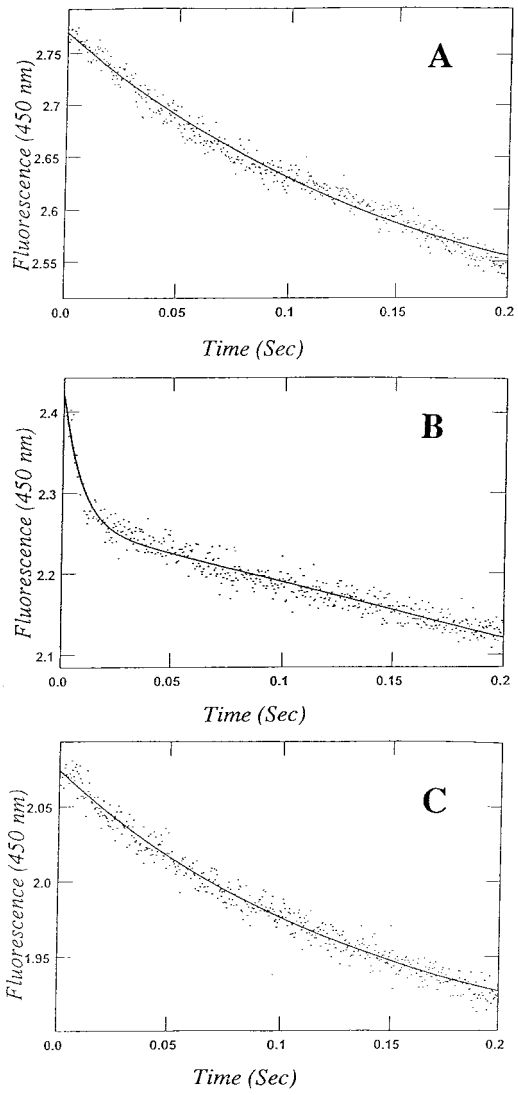

FIGURE 4: DHFR catalysis as measured by coenzyme fluorescence energy transfer. (A) A representative stopped-flow fluorescence trace shows the time-dependent formation of $NADP^+$. The trace is the change of the fluorescence signal with time after mixing a solution of bifunctional TS−DHFR (7.5 μM) preincubated with FdUMP (100 μM) and H_2folate (50 μM) with NADPH (500 μM) in the presence of $MgCl_2$ (25 mM) and EDTA (1 mM) at pH 7.8 and 25 °C. The fluorescence excitation was at 290 nm and emission at 450 nm. The data are fit to a single-exponential equation with a rate of 6.4 ± 0.3 s^{-1}. (B) A representative stopped-flow fluorescence trace shows the time-dependent formation of $NADP^+$. The trace shows the change in the fluorescence signal with time after mixing a solution of bifunctional TS−DHFR (7.5 μM) preincubated with FdUMP (100 μM), CH_2H_4folate (50 μM), and H_2folate (50 μM) with NADPH (500 μM) in the presence of $MgCl_2$ (25 mM) and EDTA (1 mM) at pH 7.8 and 25 °C. The fluorescence excitation was at 290 nm and emission at 450 nm. The data are fit to a burst equation with the rate for the fast phase of 119 ± 6 s^{-1} and for the slower phase of 9 ± 0.4 s^{-1}. Under these conditions, the chemical step rate constant is much faster than in Figure 4A. (C) A representative stopped-flow fluorescence trace shows the time-dependent formation of $NADP^+$. The trace shows the change in the fluorescence signal with time after mixing a solution of bifunctional TS−DHFR (7.5 μM) preincubated with CH_2H_4folate (50 μM) and NADPH (500 μM) with H_2folate (50 μM) and FdUMP (100 μM) in the presence of $MgCl_2$ (25 mM) and EDTA (1 mM) at pH 7.8 and 25 °C. The fluorescence excitation was at 290 nm and emission at 450 nm. The data are fit to a single-exponential equation with a rate of 7.0 ± 0.3 s^{-1}.

bated with FdUMP (100 μM) and H_2folate (50 μM) and then mixed with a saturating concentration of NADPH (500 μM) at pH 7.8. The chemical step rate in the first turnover is approximately 6.4 s^{-1} (Figure 4A). However, when the CH_2H_4folate was added to the enzyme solution, the chemical step rate for the DHFR is enhanced to 120 s^{-1} (Figure 4B). Formation of the dead end ternary complex at the TS site was confirmed by assaying the enzyme and establishing that it is unable to catalyze the TS reaction. The combination of these two experiments provides direct evidence for activation of the DHFR site via the TS site and suggests the formation of the ternary complex is a prerequisite for the catalytic enhancement. To confirm that the formation of the ternary complex was essential for activation, a third experiment was carried out in which enzyme preincubated with CH_2H_4folate and NADPH was mixed with H_2folate and FdUMP. Under these conditions, no activation of DHFR activity is observed (Figure 4C), indicating that formation of the ternary complex is required and provides additional evidence for an ordered mechanism for TS catalysis.

Reciprocal Activation of the TS Activity via the DHFR Site. Since the studies described above indicated that the formation of a ternary complex could activate the DHFR activity for the bifunctional TS−DHFR enzyme, related issues are whether ligand occupancy at the DHFR site may alter conformational changes or catalysis at the TS site which may result in differences between monofunctional and bifunctional forms of the enzyme. Recent transient kinetic analysis of the monofunctional TS suggest that a protein conformational change associated with formation of a ternary complex precedes the rate-limiting chemical step involving hydride transfer (*23*). Previous studies on the monofunctional TS enzyme have shown that the CH_2H_4folate can be used to quench the intrinsic TS fluorescence in the presence of FdUMP due to the formation of a ternary complex which is unable to undergo catalysis (*30*). Thus, the change in intrinsic fluorescence could be used to measure the rate of ternary complex formation between enzyme, FdUMP, and CH_2H_4folate at the TS active site of the bifunctional enzyme in the absence and presence of ligand(s) at the DHFR site. The experiments were performed in the presence of saturating concentrations of ligand such that binding would not be rate-limiting. A representative trace in the absence of the ligand, NADPH, displays the change in fluorescence observed after mixing a solution of enzyme and FdUMP (100 μM) with CH_2H_4folate solution (50 μM) as shown in Figure 5A. The data were fit to a single-exponential phase followed by a linear phase to obtain the rate of complex formation as 1 s^{-1} and a very slow linear rate which may indicate enzyme photobleaching. The rate of this conformational change due to complex formation in the absence of NADPH (1 s^{-1}) is relatively slow and similar to the steady-state rate which is 2.6 s^{-1}. However, as shown in Figure 5B, the rate of conformational change in the presence of NADPH (500 μM) is enhanced. The data indicate two exponential phases followed by a linear phase. The two exponential rates are 210 and 5.4 s^{-1}, respectively, and are now faster than the steady-state rate of TS. From these data, we cannot determine which rate (210 or 5.4 s^{-1}) may represent the conformational change. Although we cannot rule out the possibility that these data may reflect differences between the behavior of FdUMP and dUMP, it is more likely that

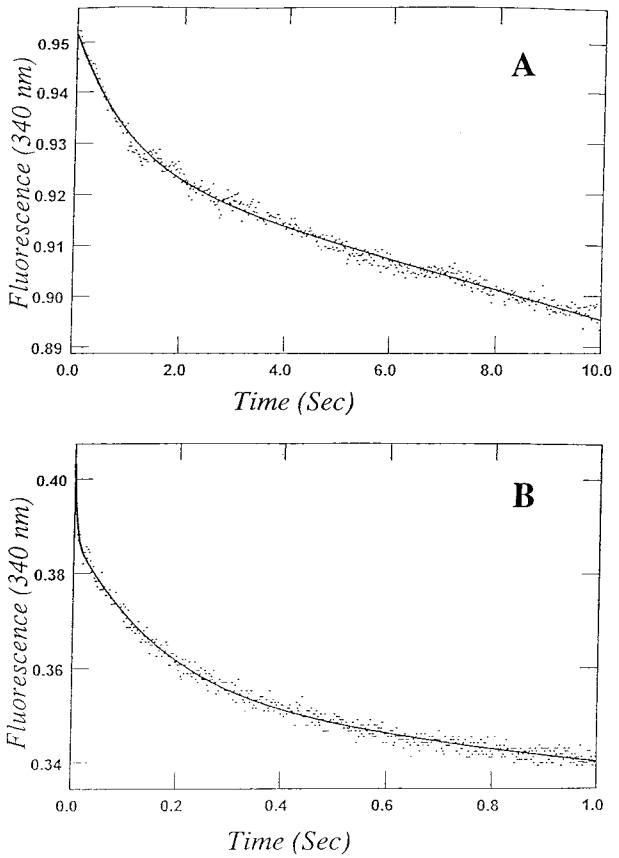

FIGURE 5: (A) Formation of the ternary complex of TS as measured by fluorescence quenching in the absence of NADPH. A representative stopped-flow fluorescence trace shows the time-dependent formation of the ternary complex of TS. The trace shows the change in the fluorescence signal with time after mixing a solution of bifunctional TS−DHFR (7.5 μM) preincubated with FdUMP (100 μM) with CH_2H_4folate (50 μM) in the presence of $MgCl_2$ (25 mM) and EDTA (1 mM) at pH 7.8 and 25 °C. The fluorescence excitation was at 287 nm and emission at 340 nm. The data are fit to a burst equation with a rate of 1.0 ± 0.03 s^{-1} for the single-exponential phase. (B) Formation of the ternary complex of TS as measured by fluorescence quenching in the presence of NADPH. A representative stopped-flow fluorescence trace shows the time-dependent formation of the ternary complex of TS. The trace is for the change of the fluorescence signal with time after mixing a solution of bifunctional TS−DHFR (7.5 μM) preincubated with FdUMP (100 μM) and NADPH (500 μM) with CH_2H_4folate (50 μM) in the presence of $MgCl_2$ (25 mM) and EDTA (1 mM) at pH 7.8 and 25 °C. The fluorescence excitation was at 287 nm and emission at 340 nm. The data are fit to a double-exponential burst equation with a rate of 210 ± 30 and 5.4 ± 0.2 s^{-1} for the faster and slower phases, respectively.

these experiments indicate reciprocal communication between the DHFR and TS active sites. Further investigation is required to understand the effects of ligand occupancy at the DHFR site upon the TS catalytic activity.

DISCUSSION

The application of rapid chemical quench and stopped-flow fluorescence methods to the study of the bifunctional TS−DHFR has allowed a direct analysis of the kinetics for the conversion of CH_2H_4folate to H_4folate. This study provides definitive evidence for the substrate channeling of H_2folate from the TS site to the DHFR site and suggests some key features of the kinetics which govern the efficient transfer between sites. The H_2folate intermediate is channeled efficiently as a consequence of at least two features of the reaction kinetics. First, the rate of H_2folate transfer from the TS site to the DHFR site is very rapid (>1000 s^{-1}) such that it does not accumulate during a single enzyme turnover. Second, the stopped-flow experiments demonstrate that DHFR catalysis is activated approximately 10-fold in the presence of the covalent ternary complex at the TS site. Likewise, NADPH bound in the DHFR site also activates TS activity. In contrast, MTX bound in the DHFR site appears to decrease TS activity and may represent an off switch for regulation of H_2folate formation at the TS site. The information gained on the reaction kinetics for H_2folate channeling and domain−domain activation is summarized in Scheme 5. The salient features of this model suggest that in the absence of ligands at the TS site (dUMP and CH_2H_4-folate) the enzyme is in a conformer with a lower specific activity. The binding of dUMP and CH_2H_4folate and formation of the covalent ternary complex result in an activation to a more active conformer. For DHFR catalysis in the absence of the ternary complex at the DHFR site, this is represented by the a pathway in which E·H_2folate·NADPH is converted to E·H_4folate·$NADP^+$ at a rate of 14 s^{-1}. In the presence of the ternary complex *E·dUMP·CH_2H_4folate at the TS site, the DHFR site is activated such that *E·H_2-folate·NADPH is converted to E·H_4folate·$NADP^+$ at a rate of 120 s^{-1}. This experiment establishes that there are domain−domain interactions between the TS and DHFR active sites. Likewise, experiments examining the formation of the covalent E·FdUMP·CH_2H_4folate ternary complex in the absence and presence of NADPH suggest reciprocal communication may also occur.

Scheme 5

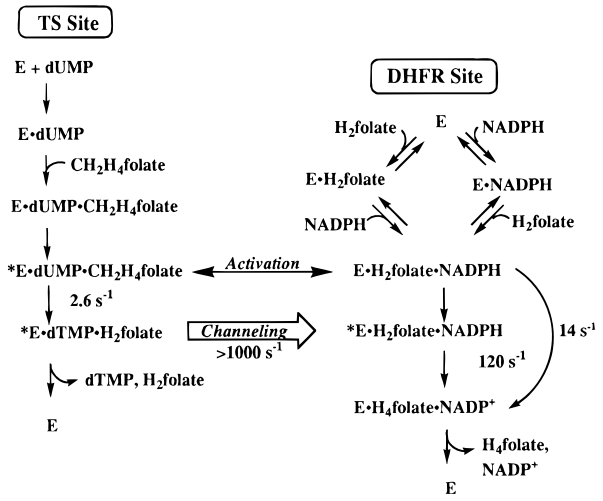

In the most active conformer under conditions of substrate channeling, H_2folate is formed at the TS (2.6 s^{-1}) and does not accumulate but rather is transferred to the DHFR site at a rate of >1000 s^{-1} without diffusion into the medium. At the DHFR site, H_2folate is rapidly converted to H_4folate (120 s^{-1}). The activation and interplay between the TS and DHFR sites are most likely modulated via changes in protein conformation and indicate that there is a tight coupling of TS−DHFR catalytic activity and that domain−domain communication is important for efficient channeling of H_2-folate.

The structural basis for TS−DHFR interdomain communication is not completely understood; however, it is

interesting to speculate on the basis of the three-dimensional structures for the bifunctional and monofunctional enzymes. Unlike its monofunctional counterparts, TS−DHFR is a bifunctional enzyme with a peptide linker connecting two existing enzymes. The DHFR domain contains an N-terminal extension which is absent in monofunctional DHFR enzymes. Earlier studies have demonstrated that there are conformational changes upon ligand binding in both of the monofunctional TS and DHFR enzymes. Therefore, it is of interest to understand similarities and differences between the two enzyme forms and how such conformational changes affect the activity and domain−domain communication in the bifunctional TS−DHFR. The structure of the *E. coli* TS covalent ternary complex shows that ligand binding causes one side of the TS enzyme to clamp down on the active site (*31*−*33*). Interestingly, much of the TS−DHFR interface in the bifunctional TS−DHFR involves residues that correspond structurally to those that move when the *E. coli* TS enzyme forms the ternary complex. Moreover, the long N-terminal extension that exists in the bifunctional TS−DHFR, compared with that in monofunctional DHFR, interacts directly with these same TS residues (*13*). The DHFR residues that would be most affected in response to the putative movements of the TS domain in TS−DHFR upon ternary complex formation would be those located in helices of αE and αF since they either directly contact the TS residues affected by ligand binding or interact with regions of the DHFR N-terminal extension which may, in turn, induce a change in conformation in response to binding at the TS active site. It has previously been shown for the monofunctional DHFR that helices αE and αF change conformation upon NADPH binding (*34*). Moreover, studies with isocitrate dehydrogenase have shown that small movements of NADPH can have large catalytic consequences (*35*).

A comparison of the kinetic and structural analyses of TS−DHFR and tryptophan synthase suggests that there may be general features which govern the channeling of substrates in multienzyme and multireaction complexes. The structures of tryptophan synthase and TS−DHFR reveal that the "channels" may be tunnels through the protein interior or pathways along the surface of the enzyme. Most recently, the crystal structure for carbamoyl phosphate synthetase, another enzyme suggested to display substrate channeling, has been solved (*2*, *36*). A channeling pathway has been proposed involving a contour length of >96 Å through which enzyme intermediates may pass to the ultimate active site which forms the product, carbamoyl phosphate (*2*, *36*). The nature of the residues that line the tunnel or pathway appears to be related directly to the physiochemical nature of the intermediate which must aid in facilitating diffusion between the two active sites.

These channels not only act to direct the complex movement of the intermediates but also aid in the signaling process between the active sites. It is becoming clear that binding of substrate at one of the active sites can apparently signal or activate the second site, before progressing with the rapid channeling of the intermediate. The "gating" role of the channel helps to maintain the precise synchrony of the reaction at multiple active sites to minimize the accumulation of the intermediate. The synchrony between active sites and the ability to channel between active sites allow the overall reaction to be well-regulated and prevent the buildup of potentially reactive, toxic, or promiscous intermediates to be released into the cytosol. Evidence is growing that substrate channeling is a general feature of biochemistry and is of fundamental importance to the overall control and catalytic efficiency of multifunctional enzymes and enzyme complexes.

ACKNOWLEDGMENT

We thank Dr. Katherine M. Welsh for helpful suggestions regarding TS−DHFR enzyme expression and purification and Dr. David A. Matthews for providing the X-ray coordinates for the bifunctional TS−DHFR and helpful comments regarding the three-dimensional structure.

SUPPORTING INFORMATION AVAILABLE

Further details about the kinetic simulation (3 pages). Ordering information is given on any current masthead page.

REFERENCES

1. Ovadi, J. (1991) *J. Theor. Biol. 152*, 1−22.
2. Anderson, K. S. (1998) *Methods Enzymol.* (in press).
3. Miles, E. W. (1995) in *Subcellular Biochemistry, Volume 24: Proteins: Structure, Function, and Protein Engineering* (Biswas, B. B., and Roy, S., Eds.) pp 207−254, Plenum Press, New York.
4. Hyde, C. C., Ahmed, S. A., Padlan, E. A., Miles, E. W., and Davies, D. R. (1988) *J. Biol. Chem. 263*, 17857−17871.
5. Anderson, K. S., Miles, E. W., and Johnson, K. A. (1991) *J. Biol. Chem. 266*, 8020−8033.
6. Lane, A., and Kirschner, K. (1991) *Biochemistry 30*, 479.
7. Brzovic, P., Ngo, K., and Dunn, M. (1992) *Biochemistry 31*, 3831.
8. McDowell, L. M., Lee, M., Schaefer, J., and Anderson, K. S. (1995) *J. Am. Chem. Soc. 117*, 12352.
9. Meek, T. D., Garvey, E. P., and Santi, D. V. (1985) *Biochemistry 24*, 678−686.
10. Grumont, R., Washtien, W. L., Caput, D., and Santi, D. V. (1986) *Proc. Natl. Acad. Sci. U.S.A. 83*, 5387−5391.
11. Grumont, R., Sirawaraporn, W., and Santi, D. V. (1988) *Biochemistry 27*, 3776−3784.
12. Stroud, R. M. (1994) *Nat. Struct. Biol. 1*, 131−134.
13. Knighton, D. R., Kan, C.-C., Howland, E., Janson, C. A., Hostomska, Z., Welsh, K. M., and Matthews, D. A. (1994) *Nat. Struct. Biol. 1*, 186−194.
14. Elcock, A. H., Potter, M. J., Matthews, D. A., Knighton, D. R., and McCammon, J. A. (1996) *J. Mol. Biol. 262*, 370.
15. Ivanetich, K. M., and Santi, D. V. (1990) *FASEB J. 4*, 1591−1597.
16. Trujillo, M., Donald, R., Roos, D., Greene, P., and Santi, D. (1996) *Biochemistry 35*, 6366−6374.
17. Mathews, C. K., and Huennekens, F. M. (1960) *J. Biol. Chem. 235*, 3304−3308.
18. Anderson, K. S., Sikorski, J. A., and Johnson, K. A. (1988) *Biochemistry 27*, 1604−1610.
19. Barshop, B. A., Wrenn, R. F., and Frieden, C. (1983) *Anal. Biochem. 130*, 134−145.
20. Anderson, K. S., Sikorski, J. A., and Johnson, K. A. (1988) *Biochemistry 27*, 7395−7406.
21. Johnson, K. A. (1992) *Enzymes 20*, 1−61.
22. Liang, P. H., and Anderson, K. S. (1998) *Biochemistry 37*, 12206−12212.
23. Spencer, H. T., Villafranca, J. E., and Appleman, J. R. (1997) *Biochemistry 36*, 4212−4222.
24. Fierke, C. A., Johnson, K. A., and Benkovic, S. J. (1987) *Biochemistry 26*, 4085−4092.
25. Anderson, K. S., and Johnson, K. A. (1990) *Chem. Rev. 90*, 1131−1149.
26. Anderson, K. S., Kim, A. Y., Quillen, J. M., Sayers, E., Yang, X. J., and Miles, E. W. (1995) *J. Biol. Chem. 270*, 29936.

27. Danenberg, P., and Danenberg, K. (1978) *Biochemistry 17*, 4018−4024.
28. Moore, M., Ahmed, F., and Dunlap, R. B. (1986) *Biochemistry 25*, 3311−3317.
29. Santi, D., McHentry, C., Raines, R., and Ivanetich, K. M. (1987) *Biochemistry 26*, 8606−8622.
30. Donato, H., Jr., Aull, J. L., Lyon, J. A., Reinsch, J. W., and Dunlap, R. B. (1976) *J. Biol. Chem. 251*, 1303−1310.
31. Matthews, D. A., Villafranca, J. E., Janson, C. A., Smith, W. W., Welsh, K., and Freer, S. (1990) *J. Mol. Biol. 214*, 937−948.
32. Stroud, R. M., and Finer-Moore, J. S. (1993) *FASEB J. 7*, 671−677.
33. Hyatt, D. C., Maley, F., and Montfort, W. R. (1997) *Biochemistry 36*, 4585−4594.
34. Filman, D. J., Bolin, J. T., Matthews, D. A., and Kraut, J. (1982) *J. Biol. Chem. 257*, 13663−13672.
35. Mesecar, A. D., Stoddard, B. L., and Koshland, D. (1997) *Science 277*, 202−206.
36. Thoden, J., Holden, H., Wesenberg, G., Raushel, F., and Rayment, I. (1997) *Biochemistry 36*, 6305.

BI9803168